Identifying the most important factors that determine fresh groundwater availability in deltaic areas

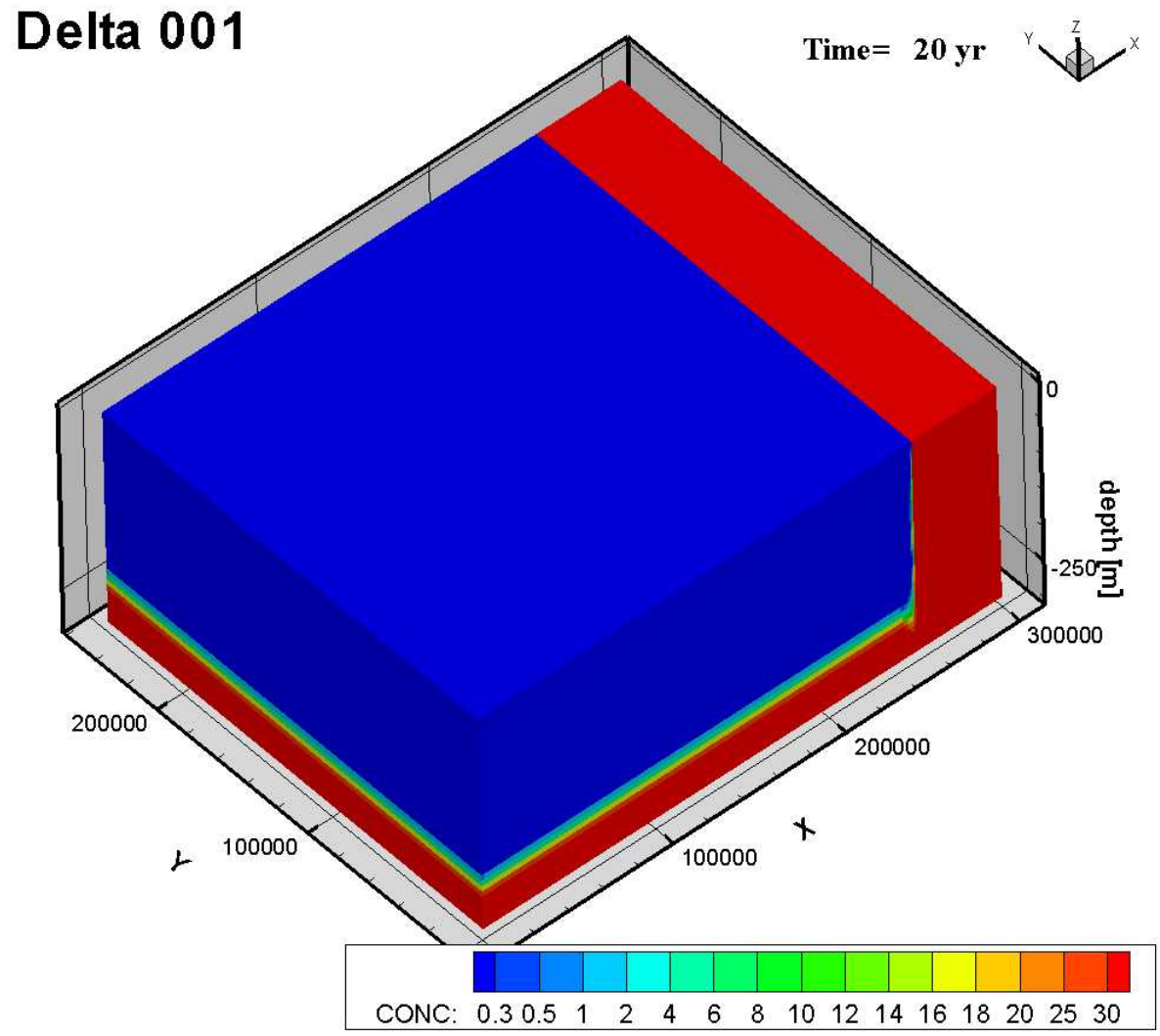

Niels Hendrikx

Identifying the most important factors that determine fresh groundwater availability in deltaic areas

Niels Hendrikx
Student Number: 3839273

A report of my research at my internship at Deltares

Internship period: April – November 2018

Supervisors:

Supervisor at Deltares: Dr. Ir. Gualbert Oude Essink
Supervisor UU: Prof. Dr. Ir. Marc Bierkens

This internship is part of the Earth Surface & Water master at Utrecht University.

Date: 10 November 2018

Table of Contents

1 Introduction

Many regions over the world experience water scarcity, driven by increasing population growth, climate change and increased irrigation rates. Over the past few decades water scarcity has become an even more widespread and serious problem. It is estimated that 800 million people lived under water stressed conditions in 1960, while in 2000 this increased to 2.6 billion (Y. Wada, van Beek, & Bierkens, 2011). During the same period of time, the usage of water has more than doubled (Y. Wada et al., 2011).

This increase in water demand leads to an increase in water supply from surface water, precipitation and groundwater. Usage of groundwater has significant advantages over usage of surface water. Firstly, groundwater is the second largest reservoir of fresh water. Secondly, groundwater is less vulnerable to contaminations and droughts compared to surface water (Custodio, 2002).
Consequently, with the doubling of water usage, the groundwater extraction rate has doubled too(Yoshihide Wada et al., 2010). Groundwater resources nowadays contribute to one third of the total groundwater withdrawal by 2010 (Y. Wada, Wisser, & Bierkens, 2014). Often, non-renewable groundwater is used; this is the amount of abstracted groundwater that exceeds the recharge.

In a study (Yoshi Wada, Van Beek, & Bierkens, 2012) it was shown that non-renewable groundwater abstraction contributes about 20% to the global irrigation demand in 2000. Furthermore, the dependency of irrigation on non-renewable groundwater increased. In addition to this, the amount of irrigation is expected to increase due to growing population numbers. Irrigation is vital for a significant amount of the total food production, up to 40%. Due to dropping groundwater levels, farmers may not be able to reach the groundwater anymore (Yoshihide Wada et al., 2012), threatening the continuity of food production in this way. In some regions, e.g. in Spain, a drawdown has been observed (Custodio, 2002) of more than 200 m.

If groundwater extraction rates continue to exceed recharge rates, depletion of groundwater occurs: the aquifer system becomes overexploited. Regions that are currently strongly affected in terms of groundwater depletion are e.g. north-west India, north-east China, north-east Pakistan, Iran, Spain, parts of the USA and the Middle East (Yoshi Wada et al., 2010).
Besides potentially threatening food production, depletion of groundwater has other serious consequences, e.g. a reduced well yield, reduced groundwater quality and a reduced base flow to surface water bodies, potentially damaging ecosystems (Konikow, 2015).
Additionally, in deltaic areas salt water intrusion may occur, resulting in the closure of wells (Barlow & Reichard, 2010; Yoshihide Wada et al., 2010). Deltaic areas that currently experience salinization problems are, for example: the Nile delta (Sherif, Sefelnasr, & Javadi, 2012), the Krishna delta (Kumar, Rao, Gupta, & Purushothaman, 2011), the Mekong delta (Minderhoud, Erkens, Pham, Vuong, & Stouthamer, 2016) and many others.

Sustainable groundwater extraction management is required to prevent and diminish the consequences of groundwater depletion and salinization to guarantee a continuous water supply. The intensity of salinization problems strongly varies among the different deltaic areas. Many factors are involved in the occurrence and evolution of salinization, e.g. amount of precipitation, abstraction amounts and geology. Simulating the evolution of salinization is often accomplished by means of a complicated numerical model. However, interpreting the results of such a complicated model and identifying the dominant physical mechanisms behind salinization may be difficult. Knowledge on this contributes to advice on sustainable pumping rates.

To improve the understanding of the dominant physical mechanisms, a synthetic groundwater model of deltaic areas was developed. However, the dominant physical mechanisms may be different depending on the area's characteristics. Based on a literature review, potentially important delta characteristics were identified. Deltaic areas can be grouped as sharing the same characteristic, e.g. geology (absence of a confining layer) or climate (high recharge).
Therefore, multiple synthetic models of deltaic areas have to be developed, of which each model is representative of (a few) real-world deltas.

To this end, a 3D synthetic groundwater model of representative deltas will be developed using iMOD-SEAWAT. Based on a literature review, a number of delta characteristics are identified and implemented in the modelling of the representative deltas like the Nile and Mekong delta. Each real-world delta will have its own characteristics with respect to for example geology, extraction rates and climate. Ideally, these delta characteristics decently resemble different real-world deltas while still retaining a schematized nature. Using these delta characteristics, the most important factors that determine fresh and brackish groundwater availability are assessed.
Ultimately, the approach will illustrate the advantage of synthetic groundwater models and lead to a better understanding of the sensitivity of fresh and brackish groundwater availability to pumping. Based on this approach, advice can be given on pumping rates (or possibly locations) for the representative delta.

2 Literature review

This section aims to give an overview of several delta characteristics, e.g. geology, climate data, abstraction data etc. This allows to group deltaic areas based on certain characteristics. Firstly, relevant data about 11 deltaic areas are summarized and subsequently presented in a factsheet format.

2.1 Overview deltaic areas

Mekong delta: it has a very thick aquitard on top which has a thickness of about 20 meter. Due to paleo regression/transgression periods, delta sediments consist of an alternation between many aquifers and aquicludes. The total thickness of all delta sediments is 600-700m. Salt water intrusion, which is seasonal in this area, covers somewhere between 15000 and 20000 km^2 (about half of the total area) during its maximum extend (Minderhoud et al., 2016). Only the upper part of the delta has fresh groundwater in at least the upper 70 meters. In the lower part all tubewells within 10-70 meters depth measured saline groundwater (Buschmann et al., 2008), sometimes with a concentration of more than 10 g/L. Rainfall amounts vary throughout the delta in the range of 1600-2400 mm/yr. This delta has a dense network of channels. The daily abstraction rate is 2.5 million m^3/day.

Red River delta: this delta has an unconfined aquifer with a thickness of about 20 m on top (Bui et al., 2011). Aquifers are recharged because they are connected to the river due to erosion. Rainfall and irrigation also contribute to aquifer recharge. The total thickness of delta sediments is about 100 m. Precipitation is on average 1600 mm/yr and it has quite an extensive river network. The delta covers an area of about 13000 m^2. In the capital city Hanoi, almost the complete water supply depends on groundwater.

Krishna delta: a small aquitard is situated on top with a thickness of about 5 meters. A chemical analysis pointed out (Kumar et al., 2011) that the groundwater has a long residence time in the deeper aquifers. This means that deeper and more landward aquifers are disconnected from the sea and the shallow aquifers. These particular aquifers also contain fresh water. Upper aquifers are recharged by rivers and in some areas also by precipitation. Refreshing of aquifers is occurring due to irrigation using an intensive canal network. A salinity front is present at 25, 30 and 50 km landward in respectively shallow, intermediate and deeper aquifers (Kumar et al., 2011). Precipitation rate is 1250 mm/yr.

Indus delta: aquifer with very high conductivites, multiple smaller discontinuous aquitards (due to silts) within aquifer. Salinization occurs over the full aquifer depth of 200 m and intrudes landward over the whole aquifer. Recharge of the aquifer is mainly by rivers, resulting in fresh water lenses around the rivers. Annual precipitation is small, ranging between 250 and 500 mm/yr. Abstraction is not evenly but more locally (focussed) distributed. In high abstraction areas in the north-western part of India, groundwater levels can drop to 20 to 50 meters below ground level (MacDonald, 2013).

Ganges Bhramaputra delta: aquifer with very high conductivities, multiple smaller discontinuous aquitards (due to silts) within aquifer. Recharge mainly by rainfall. Salinization is highly seasonal. The vertical extend of the aquifer system is a few hundreds of meters (Hoque, Burgess, Shamsudduha, & Ahmed, 2011). The basin can be divided in two parts,

based on hydrostratigraphic arguments: the southern part can be considered a multi-aquifer system, while the northern part is a single-aquifer system (Mahmud, Sultana, Hasan, & Ahmed, 2017).
Deeper aquifers do not receive any modern recharge and the chemical composition did not change after two to four decades of pumping. In general, the deeper aquifers are resilient to climate or pumping induced changes (MacDonald, 2013).

Niger delta: in the inland part of the delta the two major aquifers in this delta are unconfined. More towards the coast, the aquifers become confined. Towards the inland the aquifers increase in thickness, while on the other hand the confining layers become smaller and disappear. Regions with confined aquifers are characterized by having artesian flows. Both aquifers are highly permeable and only in the southern part low permeable layers are present. The aquifer system reaches a depth of a few hundreds of meters. In the Niger delta the amount of recharge is very high, ranging from 2400 mm/yr up to 4800 mm/yr at the coast (Goni et al., 2008). This delta is characterized by a dense river-creek network. Due to high recharge amounts and additional recharge by the river, groundwater levels are very shallow. In the city Port Harcourt, which is located in the delta, the annual abstraction rate was(Abam, 2001) at most 4 km^3/yr.

Yangtze delta: In this delta five aquifers are present, one unconfined aquifer that is situated on top, and four confined aquifers that are being alternated with aquitards. The total thickness of sediments overlying the bedrock varies from 100 to 360 meters (Zhang et al., 2007). Groundwater pumpage rates cause land subsidence (Zhu, Wu, Wu, & Ye, 2011): in these areas the abstraction rate is approximately 10^6 m^3/day. Also recharge by the river. Precipitation and hence recharge to the aquifer is seasonal but the annual precipitation varies from 1000 to 1500 mm/yr. Both groundwater pumpage and recharge to the groundwater cause groundwater levels to fluctuate too.

Mahamadi delta: in the upper part of the delta, one unconfined aquifer is situated on top and one confined aquifer below. The lower aquifer is underlain by bedrock, acting as aquifer base (Sahoo & Jha, 2017). In the upper part of the delta, the total thickness of the aquifer system is around 100 meters, increasing towards the lower delta where the aquifer system reaches it maximum thickness of 600 meters. Annual precipitation in this area is 1400 mm and consequently, aquifer recharge is mainly by rainfall (70%). Other smaller components that contribute to aquifer recharge are: irrigation, seepage from water bodies etc. The fresh/salt water distribution is strongly spatially dependent. In the upper part of the delta, only fresh water aquifers are present. In other parts, saline groundwater is present in deeper aquifers, with fresh water on top. However, other areas are characterized by having aquifers with saline groundwater on top, while deeper aquifers bare fresh groundwater (Radhakrishna, 2001). The highest transmissivities are found in the aquifers in the upper delta: up to 4500 m^2/day.

Po delta: the upper aquifer in the southern part of the delta is unconfined, in general. This aquifer is mainly recharged by dune and paleodune systems, while on the other hand it discharges to surface water network that are being drained (Colombani, Cuoco, & Mastrocicco, 2017). In general freshwater is found in the upper part of the aquifer, while in the basal part, hypersaline groundwater is found.
sea water intrusion. It was observed that in more than half of the groundwater samples in this particular area, very high salinity values were present. A chemical analysis pointed out that

this is due to evapotranspiration. Rainfall has only a small contribution to aquifer recharge, since the average annual precipitation is around 600 mm/yr (Antonellini et al., 2008).

Rhone delta: in the Holocenic deposits, two aquifers are present. On top is an unconfined aquifer, which contains very saline water and soil in the southern part of the delta. The deeper aquifer is disconnected from seawater due to a confining layer, limiting seawater intrusion in this way. East of the river, the deeper aquifer, which outcrops there, is used for drinking water supply and industry. In the eastern part, this aquifer receives twice as much artificial recharge by means of irrigation compared to rainfall, which is approximately 600 mm/yr. West of the river, this aquifer is saline but east of the river it bares freshwater. Since the 1970s seawater intrusion has occurred, increasing salinity values in the deeper aquifer (de Montety et al., 2008).

Nile delta: it is a semi-confined aquifer system with a maximum thickness of 900 m. The aquifer system is mostly a leaky aquifer, with smaller parts towards the western and eastern edge being unconfined. Due to a very wide and deep exposure to the Meditterean sea, severe saltwater intrusion takes place. Recharge of the aquifer system occurs by river seepage and artificial recharge (irrigation). Transmissivity values of up to 15000 m^2/day are observed, along with hydraulic conductivites between 70 and 100 m/day (Sherif et al., 2012). At depth of 170-225 m, sea water intrusion occurs as far as 100 km landward. More towards the apex of the delta, the fresh water layer has an average thickness of 200 m. As of 2010, annual groundwater abstractions in the Nile delta are (Arabi, 2012) 4.6 km^3/yr. Precipitation rates are small, it is a very dry area with at most 200 mm/yr in the northern part of the delta.

3 Methods

Based on the delta characteristics presented in the literature review, it was decided to investigate the influence of the following factors:

- Hydraulic resistance of the confining layer
- Distance from the extraction locations (e.g. a city) to the sea
- Amount of extraction
- Spatial distribution of extractions
- Initial fresh/salt water interface depth
- Recharge
- Presence of an additional clay layer

Other potentially important factors, e.g. sea level rise, presence of mountainous areas, leakiness of aquifers are not discussed.

The influence of these factors is investigated by means of a synthetic delta groundwater model that was developed during this project. Since deltaic areas are confronted with salt water intrusion, the variable density groundwater flow model iMOD-SEAWAT is used. Before elaborating on the procedure of investigating the influence of aforementioned factors, the set-up of the conceptual model is discussed.

3.1 Model dimensions

In line with the idea of a conceptual model, the synthetic delta area is assumed to be simply rectangular. In Figure 1, the model area is viewed from top, with a length L of 300 km, width W of 250 km and a depth of 300 m. The seaward area has a length of 50 km, hence the deltaic part of the area comprises 62500 km^2. Real deltaic areas vary greatly in size, ranging from about 1000 km^2 to more than 100000 km^2. This implies that the synthetic delta is relatively large but it is not among the largest deltas.

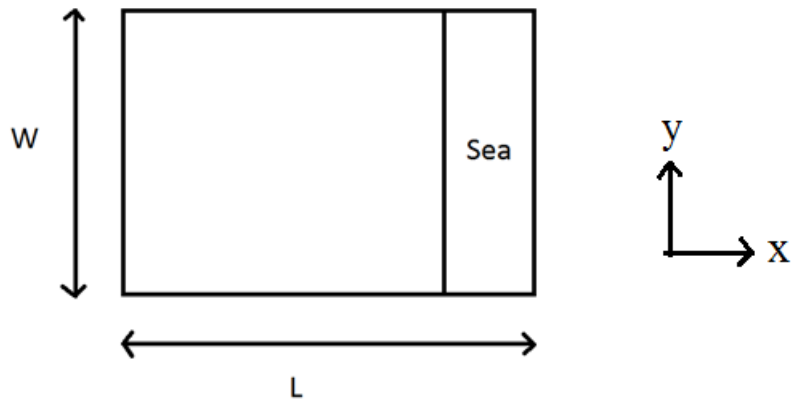

Figure 1: model area viewed from top.

3.2 Geology

The model consists of four layers: two aquitards and two aquifers. In Figure 2 an outline of this simple geology is presented. Furthermore, the topography of the synthetic delta is assumed to be perfectly flat, which is not a very strong simplification considering that deltaic areas are quite flat in general. Furthermore, the porosity is assumed to be 0.3 for all layers and the storage coefficient is 0.0005, except for the upper layer where it is 0.15. The upper layer acts as a confining layer and its thickness will be varied. For simplicity, it is assumed that every layer is vertically and horizontally homogeneous. This implies that the horizontal and vertical hydraulic conductivity of each layer can both be described by a constant. The values are specified in the table below:

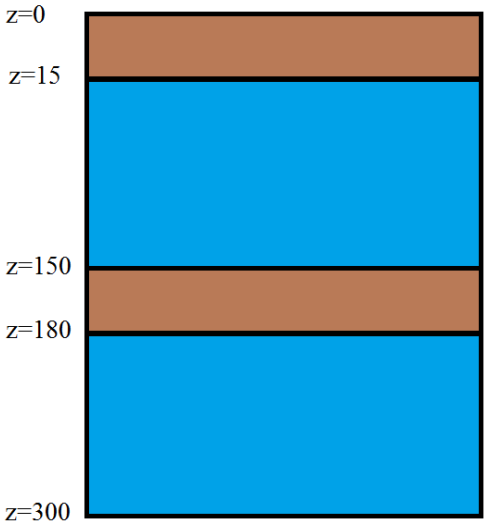

Figure 2: outline of the model geology with depth in meters. Brown areas indicate aquitards, while blue areas represent aquifers.

Layer	1	2	3	4
K_H (m/day)	0.01	50.0	0.01	50.0
K_V (m/day)	0.001	5.0	0.001	5.0
T (m^2/day)	<1	6750	<1	6000

Both aquifers have fairly high transmissivities but this is not unusual; e.g. in the Nile delta transmissivities are found of up to 15000 m^2/day.

3.3 Spatial and temporal discretization

A relatively coarse grid size of 1 km x 1 km is used because this research focusses on global rather than local effects. Another advantage is that run-time is relatively short.
Vertically a grid size of 7.5 meters is used. The vertical discretization is much finer because the process of upconing of saline groundwater has to be captured.

During the first 100 years of simulating, a time-step of one year is used, while in the successive 100 years of simulated time, the time-step is increased to two years.

3.4 Rivers & Drains

Two big rivers without any major tributaries are implemented. This of course is a major simplification but this approximation is in line with the idea of a conceptual model. Furthermore, in every grid cell ditches are present. In Figure 3 an outline of the model area is

given, viewed from top. The two big rivers are directly connected to the aquifer below the confining layer, whereas the ditches are not.

The impact of both the rivers and ditches on the hydrology can be varied by means of the conductance (McDonald & Harbaugh, 1988):

$$COND = \frac{KLW}{M}$$

with K the streambed hydraulic conductivity of the river/ditch, L the length, W the width and M the riverbed thickness. The conductance depends on the spatial discretization. In this case, the horizontal discretization is 1 km by 1 km. Consequently, the maximum value for L will be 1 km, which means the rivers length within the gridcell is 1 km. For the two big rivers a width of W= 100 m is used. Naturally, the width of ditches will be much smaller but in one gridcell many ditches can be present. To account for this, the width of all ditches is added and therefore the width for ditches is set to W= 200 m.

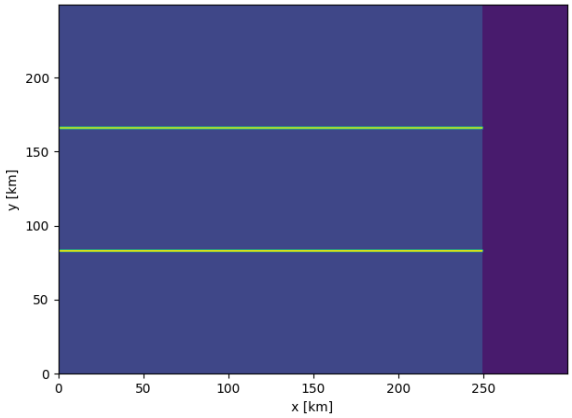

Figure 3: the domain viewed from top. In yellow the two big rivers are depicted, purple indicates the sea and the darkblue area the land.

In this way, the extent of the river network can be varied in accordance with different climate scenarios: dry, with less ditches/smaller rivers or humid with more ditches and bigger rivers/tributaries.

Often, the streambed conductance is used, defined as c = M/K to compute the river conductance. Apart from river length and width, the streambed conductance is harder to measure and it can vary by orders of magnitude.
For simplicity the streambed conductance is assumed to be constant throughout the river. In reality however, it is spatially dependent(Lackey, Neupauer, & Pitlick, 2015). For example, the streambed hydraulic conductivity depends on many geological and hydrological factors(Naganna, Deka, Ch, & Hansen, 2017), e.g. size and density of suspended sediment. The hydraulic conductivity can range from 10^{-6} – 10^{-8} m/s for a loamy type of soil to highly permeable with more than 10^{-4} m/s for sands and gravels with low fine-grained fraction(Naganna et al., 2017). For this reason, the hydraulic conductivity of the riverbed will be set to K= 0.1 m/day and of the streambed of ditches it will be smaller with 0.004 m/day. Since the conductivity strongly varies, the streambed thickness is set for both rivers and ditches to 0.5 m for simplicity. The values used to compute the conductance of the rivers and ditches in the reference scenario are given in the table below:

	L (m)	W (m)	c (day)	RIV_COND
Rivers	1000	100	5	20000
Ditches	1000	200	100	1000

3.5 Recharge

For our reference scenario, the upper aquifer receives 1 mm/day of recharge. Since only a part of the rainfall ends up in the aquifer, the total amount of rainfall the area receives is at least twice the amount of recharge. Estimations of the ratio between precipitation and recharge vary highly according to model results(Jasechko, 2014), on average recharge was 16% of the annual precipitation. In a study(Kotchoni et al., 2018) where groundwater recharge in aquifers was estimated, showed a strong dependence on aquifer type. Annual recharge ranged from 4% to 40% for shallow Quarternary sandy aquifers. Choosing our recharge to be 40% of the annual precipitation, our reference scenario will receive roughly 900 mm/yr. In a few scenarios, recharge is doubled, corresponding to a humid area, whereas in other scenarios it is halved, corresponding to an (semi-) arid area.

3.6 Initial conditions

The model has to be initialized in terms of hydraulic head and concentration. The following hydraulic head distribution is used:

$$h(x) = 30\left(1 - \frac{x}{250}\right), \qquad 0 \leq x \leq 250$$
$$h(x) = 0, \qquad 250 > x \geq 300.$$

This very simple distribution, visualized in Figure 4, has a horizontal gradient, generating a small regional flow, with no y-dependence. In our conceptual model a general density gradient exists from fresh water (C_0 = 0 g/L) in vicinity of the surface towards saline groundwater (C_0 = 35 g/L) at the bottom. Saline and fresh groundwater is separated by an interface with a thickness of 7.5 meters which has a concentration of C_0 = 17.5 g/L. The depth of the initial location of this interface varies with scenario. However, the scenarios cannot yet be simulated with these initial conditions.

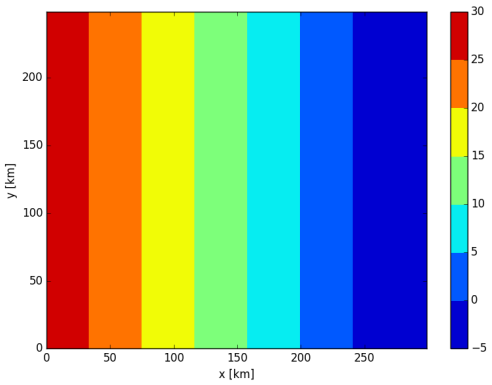

Figure 4: initial hydraulic head distribution, expressed in meters. On the right is the seaward side, with h=0 m.

In the first place, the model has to determine a steady state with respect to hydraulic head and fresh/salt water distribution. To this end, the evolution of fresh/salt water distribution is simulated for 150 years. It is important to note that at this stage, no wells are activated yet. In this way, the natural fresh/salt water distribution can be established. Afterwards, this final distribution of fresh/salt water is used as initial condition for the accompanying scenarios.

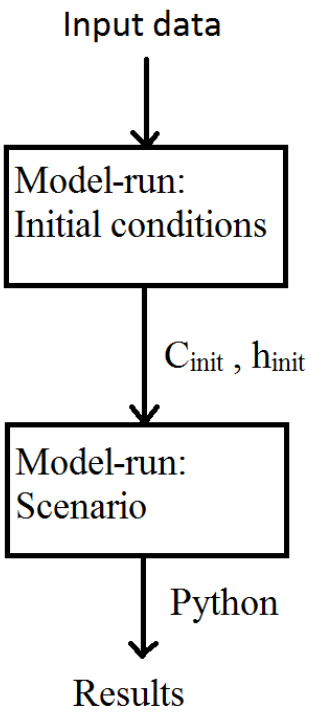

Figure 5: model flow diagram

Schematically, the procedure to set up and run the different scenarios is visualized in Figure 5. Firstly, the initial conditions are prepared by providing an initial concentration and head distribution. Secondly, the model determines an approximate steady state with respect to both fresh/salt and head distribution. Thirdly, this distribution of both concentration and head is used for the simulation of the scenarios.

3.7 Boundary conditions

At the edges of the conceptual model, boundary conditions have to be prescribed in terms of hydraulic head and solute concentration. At the seaward side, on the right in Figure 6, the concentration at model layer K=1 is fixed at C_0 = 35 g/L and the hydraulic head is fixed at h=0. Every grid cell representing the sea is of general head boundary type (GHB), see appendix B. In addition to this, for every layer, all grid cells on the edge have the GHB type. At depth on the seaward side, comprising the area where ($250 < x < 300$, $0 < y < 200$), i.e. for K>1,

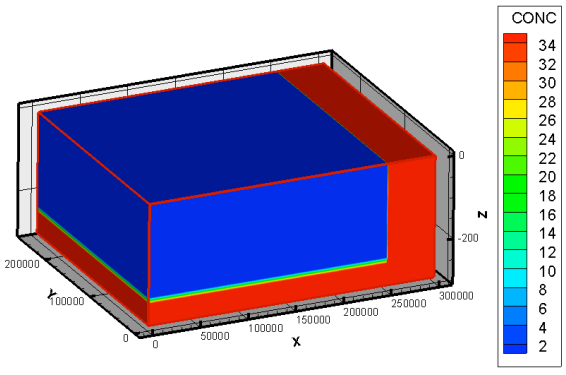

Figure 6: initial concentration distribution, in g/L. On the r.h.s. the sea is present. On the landward side, the saline groundwater is located at z=240 m in this example. Distances are expressed in meters.

both the concentration and hydraulic head are fixed only on the edges and not in the interior. This allows the fresh/salt interface in the vicinity of the sea to rotate and develop freely. Hydraulic heads are prescribed on the edges in such a way that a small horizontal gradient is imposed:

$$h(x) = 30\left(1 - \frac{x}{250}\right), \qquad 0 \le x \le 250.$$

While the boundary at (x=0,y) has a clear physical interpretation, i.e. connecting the delta with the hinterland, the other two boundaries (x,y=0) and (x,y=W) are less straightforward. In this case, the delta represents a slice of land taken out of a long coast. Since the two boundaries connect the delta to land, it is assumed fresh water enters the delta from both

sides. Each of the boundaries (x=0,y),(x,y=0) and (x,y=W) are represented with the general head boundary type. The conductance of both the land and seaward boundaries is set to at least 10^9 to maintain the prescribed hydraulic heads.

Since a density gradient over depth exists due to increasing salt concentration, the prescribed hydraulic heads should be corrected for this (Post, Kooi, & Simmons, 2007), otherwise no hydrostatic conditions are achieved. At depths where fresh groundwater is prescribed, a density of 1000 kg/m3 is prescribed. If the concentration changes, the density and hydraulic head change accordingly, for example:

Salinity	Depth (m)	Concentration (g/L)	Hydraulic head (m)	Density (kg/m^3)
Fresh	0-232.5	0	30	1000
Brackish	232.5-240	17.5	26.8	1012.5
Saline	240-300	35	23.5	1025

The concentration as function of depth varies depending on the scenario and consequently, the prescribed hydraulic heads change too.
As already explained in the previous section, the initial conditions for the scenarios have to be prepared: an approximate steady state with respect to fresh/salt water distribution and hydraulic head has to be reached. For this, the boundary conditions described in this section are used. However, after the steady state is reached, a small mismatch arises between the steady state of the interior and the boundary conditions in terms of salt concentration. The model tends to smooth the interface more out over a greater vertical distance. Ultimately, an iterative process can be used to match the boundary conditions with the steady fresh/salt water distribution of the interior. However, with regards to time schedule, this iterative process is omitted. In other words, the original boundary conditions used for the preparation of the initial conditions are also used to simulate the scenarios.

3.8 Pumping well

Pumping of groundwater by cities is highly schematized in this project. A city is represented by a circular area with a radius *R* and within this area all pumping wells are located.
All wells are distributed over this circular area. This can be either randomly (Figure 7), or for example, with increasing density towards the centre of the circular area (Figure 8). The latter is an attempt to simulate a more densely populated city centre.

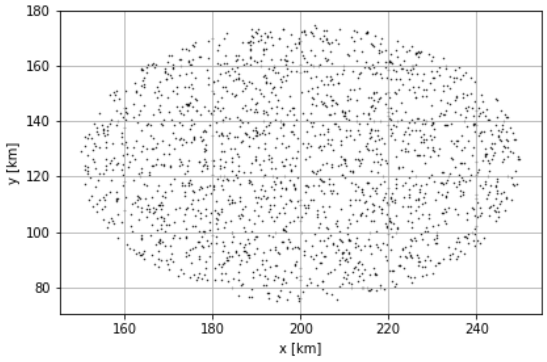

Figure 7: location of the city, each dot represents a well. All wells are randomly distributed within the city.

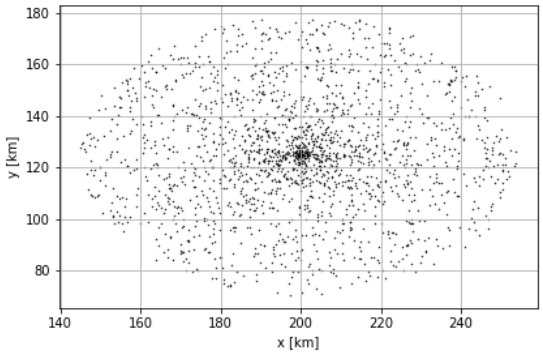

Figure 8: location of the city, each dot represents a well. In this case the wells are more clustered in the city centre.

In the first example, well positions are chosen randomly within a squared area and only the wells that are situated within a circle with radius *R* and centre ($x_0 = 200$, $y_0 = 125$) are retained. In the latter example, Figure 8, for each well a random angle (θ) and radius (R) is chosen. Consequently, the position of the wells is determined by:

$$x = x_0 + R \sin\theta$$
$$y = y_0 + R \cos\theta$$

Subsequently, the total abstraction rate and the amount of wells had to be determined. From the literature review a great range in yearly groundwater abstractions was found among the different deltaic areas. Since each delta has a different annual abstraction rate and area, the average abstraction per unit area Q_a :

$$Q_a = \frac{Q_{tot}}{A}$$

varies too, with Q_a expressed in $m^3/day/km^2$. Abstraction rates have been mapped globally(Yoshihide Wada et al., 2010), often expressed in mm/yr. In the year 2000 high abstraction rates were found in India, Bangladesh, China, Egypt, Europe and the USA of up to 1000 mm/yr, or approximately 2700 $m^3/day/km^2$. For our reference scenario, we chose the total annual abstraction rate to be Q_{tot} = 3 km^3/yr, which corresponds to approximately Q_a=1000 $m^3/day/km^2$. Hence, this amount of abstraction is still far away from the high end abstractions. Therefore, starting from the reference scenario, the influence of both a decrease and an increase in abstractions can be tested. The last decision to be made was with regard to the number of wells. Since the abstractions will take place over a circular area, representing an urban area, with $A = \pi r^2$ and r = 50 km, the total area is approximately 8000 km^2. Furthermore, each gridcell covers an area of 1 km^2, 8000 wells will be used. This corresponds to a moderate to high well yield of 11.5 l/s.

3.9 Dispersivity

Two values of the longitudinal dispersivity have been tested: 1 m/day and 10 m/day. For the scenarios, which are described in the next section, the initial depth of the saline groundwater is respectively 240, 180 and 120 m. At a depth of respectively 225, 165 and 105 m, the groundwater was perfectly fresh again (C=0 g/L).

To test the influence of dispersivity, the initial fresh/salt water interface was placed at a depth of, e.g., 240 m. Subsequently, the movement of the interface was monitored for the two dispersivity values. For α_L= 10 m/day, saline groundwater (corresponding to a concentration of more than 1 g/L) vertically extends about 60 meters above the original location of the fresh/salt water interface after 150 years. On the other hand, if α_L = 1 m/day, this is reduced to 22.5 – 30 meters. Consequently, after the approximate steady state was reached, the saline groundwater (with C> 1 g/L) reached a depth of respectively 217.5, 172.5 and 90 m. Therefore α_L = 1 m/day was selected for all model computations.

3.10 Scenarios

The amount of water that can be extracted depends on many factors. To identify the separate influence of each factor, a number of scenarios were developed. Each scenario corresponds to a different combination of parameters, initial conditions and pumping management. All scenarios are simulated for an initial interface depth of respectively 240,180 and 120 m. The most basic scenario, 000, 100 and 200, do not simulate any wells. The first scenarios that do include wells are 001,101 and 201. From now onwards, these scenarios are referred to as ‘reference scenarios’. Any next scenario has one different setting compared to scenario 001 and 101. In this way, it is attempted to isolate the influence of the particular setting being adjusted.

In a few scenarios multiple settings are changed simultaneously. This can be justified in the following way, e.g. adjusting annual recharge amounts will also affect the river network. In regions that receive high annual recharge amounts, a more extensive river network is required to drain the area. One way to control the extent of the river network is to vary river conductance. Hence, in scenarios 7-10 where the annual recharge is varied, river conductance varies in a corresponding way. In other words, if annual recharge increases, more water has to be drained by the rivers, which requires a higher river conductance.

Below, an overview is given of all scenarios. Each setting or parameter that is changed with respect to a reference scenario (001, 101, 201) is indicated with a red color.

Overview of all scenario properties:

Scenario	**000**	**001**	**002**	**003**	**004**	**005**
C (day)	15000	15000	15000	15000	15000	1500
Number of aquitards	1	1	1	1	1	1
L_x (m)	-	50	50	50	100	50
Well distribution	-	R	F	R	R	R
Q_{tot} (km^3/yr)	0	3	3	0.3	3	3
z_I (m)	240	240	240	240	240	240
Recharge (mm/yr)	365	365	365	365	365	365
RIV_COND	1000; 20000	1000; 20000	1000; 20000	1000; 20000	1000; 20000	1000; 20000

Scenario	**006**	**007**	**008**	**009**	**010**
C (day)	15000	15000	15000	1500	5000
Number of aquitards	2	1	1	1	1
L_x (m)	50	50	50	50	50
Well distribution	R	R	R	R	R
Q_{tot} (km^3/yr)	3	3	3	3	3
z_I (m)	240	240	240	240	240
Recharge (mm/yr)	365	182.5	730	730	730
RIV_COND	1000; 20000	200; 10000	4000; 80000	4000; 80000	4000; 80000

Scenario	**100**	**101**	**102**	**103**	**104**	**105**
C (days)	15000	15000	15000	15000	15000	1500
Number of aquitards	1	1	1	1	1	1
L_x (m)	-	50	50	50	100	50
Well distribution	-	R	F	R	R	R
Q_{tot} (km^3/yr)	0	3	3	0.3	3	3
z_I (m)	180	180	180	180	180	180
Recharge (mm/yr)	365	365	365	365	365	365
RIV_COND	1000; 20000	1000; 20000	1000; 20000	1000; 20000	1000; 20000	1000; 20000

Scenario	**106**	**107**	**108**	**109**	**110**
C (days)	15000	15000	15000	1500	5000
Number of aquitards	2	1	1	1	1
L_x (m)	50	50	50	50	50
Well distribution	R	R	R	R	R
Q_{tot} (km^3/yr)	3	3	3	3	3
z_I (m)	180	180	180	180	180
Recharge (mm/yr)	365	182.5	730	730	730
RIV_COND	1000; 20000	200; 10000	4000; 80000	4000; 80000	4000; 80000

Scenario	**200**	**201**	**202**	**203**	**205**	**206**	**208**
C (days)	15000	15000	15000	15000	1500	15000	15000
Number of aquitards	1	1	1	1	1	2	1
L_x (m)	-	50	50	50	50	50	50
Well distribution	-	R	F	R	R	R	R
Q_{tot} (km^3/yr)	0	3	3	0.3	3	3	3
z_I (m)	180	180	180	180	180	180	180
Recharge (mm/yr)	365	365	365	365	365	365	730
RIV_COND	1000; 20000	1000; 20000	1000; 20000	1000; 20000	1000; 20000	1000; 20000	4000; 80000

Meaning of symbols:

C: hydraulic resistance, computed with $C = \Delta Z/K_v$, with ΔZ the thickness of the confining layer. C is a measure of permeability.
L_x: distance from the city centre to the sea
Well distribution: either randomly, indicated by R, or focussed, to represent a city center, indicated by F.
Q_{tot} : combined yearly discharge of all wells.
z_I : initial depth of the fresh/salt water interface
Recharge: part of the recharge that actually recharges the aquifer (i.e. the part that does not evaporates or is used by vegetation)
RIV_COND : the first value indicates the conductance of ditches, the second represents the conductance of the big rivers.

4 Results

The results to be presented are in the form of temporal evolution of fresh water volume and number of fresh water wells still in operation. For the determination of fresh water volume the spatial distribution of concentration is used. However, only the area below the city is considered in the computation of the fresh groundwater volume.

The amount of fresh water wells is determined by checking the concentration after each stress period. If the concentration exceeds 1 g/L, the well in consideration is no longer labelled as fresh water well. However, in all scenarios the wells keep extracting water even if they pump fresh water. Since in reality these wells will obviously be closed, this does not happen in this simple model. Hence, the results have more qualitative value rather than quantitative. However, in one scenario the wells were turned off after saline groundwater was extracted. The characteristics of this scenario (201) are given in the 'Scenarios' section under Methods. In Figure 9 the number of fresh water wells over time is presented. In one scenario the wells will always continue pumping while in the other scenario they are turned off the moment saline groundwater is encountered.

From Figure 9 it becomes clear that the salinization problem is delayed if wells are turned off. However, with this delay comes also a drop in groundwater uptake. A drop of 60% in fresh water wells by 2200 corresponds to a drop in groundwater uptake of 1.8 km^3/yr (60% of 3 km^3/yr).

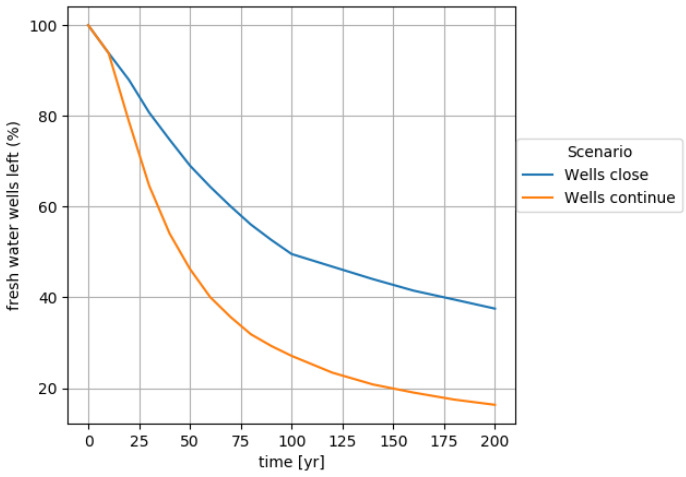

Figure 9: reference scenario for z=120 m, in one case wells continue pumping, in the other wells are turned off the moment they pump saline groundwater.

The results are subdivided in themes, each theme representing one of the factors that were assessed to have an important influence on fresh/salt distribution.

4.1 Influence of the confining layer

The first factor to be examined is (the absence of) a confining layer. One way to vary the influence of the confining layer is to adjust its hydraulic resistance. As mentioned before, the hydraulic resistance takes into account both the thickness of the confining layer, as well the vertical hydraulic conductivity. A high value of the hydraulic resistance (C), which is measured in days, indicates that a solute will take a long time to travel through this layer. The influence of the hydraulic resistance of the confining layer is investigated for a starting depth of the interface at both 240 m and 180 m. In Figure 10 and Figure 11 the influence of the confining layer on the fresh water volume is presented. Furthermore, in Figure 12 and Figure 13 the influence on the amount of fresh water wells is shown for depths of the initial interface of respectively 240 and 180 m.

For a depth of 240 m, the differences between a firm confining layer (C=15000 days) and a better permeable one (C=1500 days) are relatively small over the course of 200 years. However, already at an interface depth of 180 m, the differences become more pronounced, especially after 200 years. If the saline groundwater is located very deeply, its movement reacts weakly on changes in the configuration of the confining layer. It seems to be disconnected from conditions in the top layer to some extent.

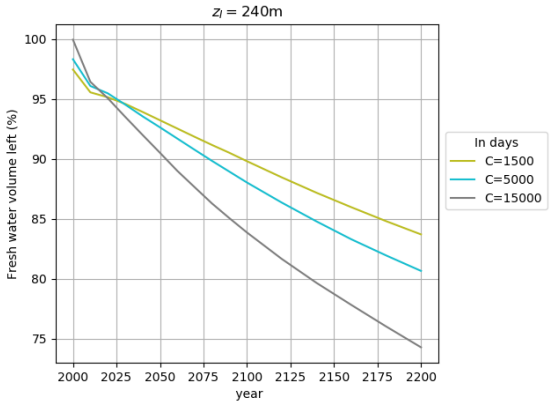

Figure 10: the influence of the confining layer on the fresh water volume is tested by varying its hydraulic resistance to vertical flow.

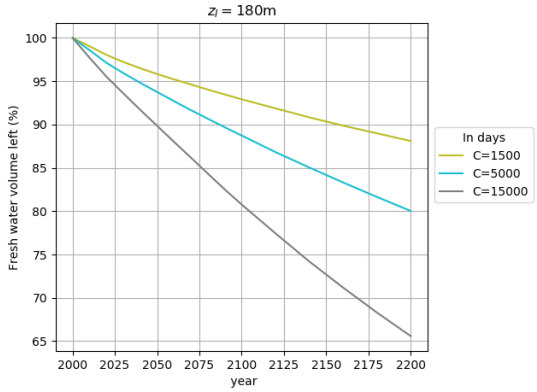

Figure 11: the influence of the confining layer on the fresh water volume is tested by varying its hydraulic resistance to vertical flow.

This is also visible in the time evolution of the amount of fresh water wells for different values of the hydraulic resistance. In the first case, Figure 12, the amount of fresh water wells is insensitive to changes in the confining layer. Even for an initial interface depth of 180 m, the difference between the three scenarios is at most 8%.

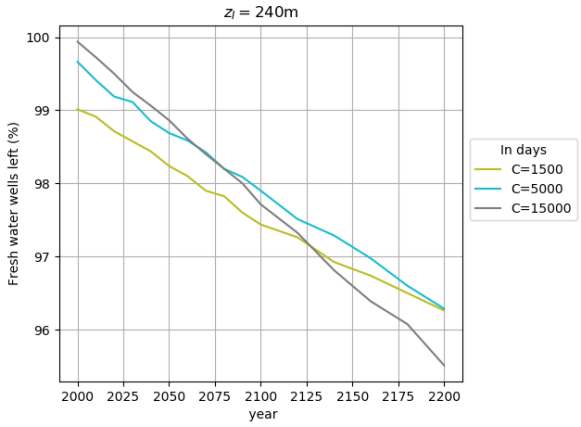

Figure 12: the influence of the confining layer on the amount of fresh water wells, the initial interface starts at a depth of 240 m.

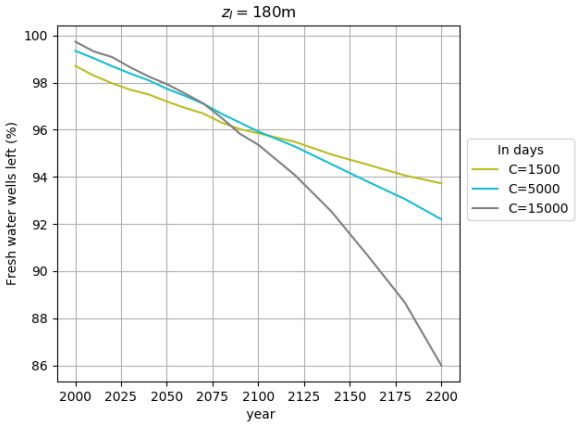

Figure 13: the influence of the confining layer on the amount of fresh water wells, the initial interface starts at a depth of 180 m.

From the water budget provided by iMOD-SEWAT it appeared that in both cases of z=240 and z=180 m, the amount of water infiltrated by rivers doubled, if the hydraulic resistance was changed from C=15000 to C=1500.

4.2 Influence of abstraction rate

Intuitively, the amount of abstraction will strongly determine the evolution of the amount of fresh water. In Figure 14 and Figure 15 the fresh water volume is plotted versus time for different abstraction rates. For Q=0, the amount of fresh water also decreases over time. This is because the initial fresh/salt distribution (before applying abstractions) has not reached a perfect steady state yet. The jumps at 2090 and 2190 are caused by discretization and definition of fresh water volume. Since the fresh/salt distribution has not reached a steady state yet, the saline groundwater slowly continues to prograde upwards. The vertical discretization is 7.5 meters. Since a grid cell only contains fresh water if the concentration is less than 1 g/L, it is either fresh or salt. For Q=0 in 2090, the concentration in one of the layers exceeds 1 g/L. This results in a relatively sudden drop in the fresh water volume. If a finer vertical discretization was used, this sudden drop would not be visible. In this case 40 model layers are used of 7.5 m, with each layer holding 2.5% of the total volume of fresh water at the start. Instead, if 400 model layers of each 0.75 m thickness, each layer only holds 0.25% of the fresh water volume. This greatly reduces the relative impact of the salinization of one model layer.

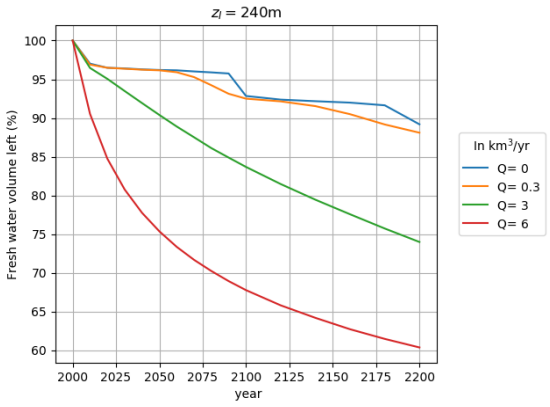

Figure 14: temporal evolution of fresh water volume for different extraction rates. The interface starts at 240 m.

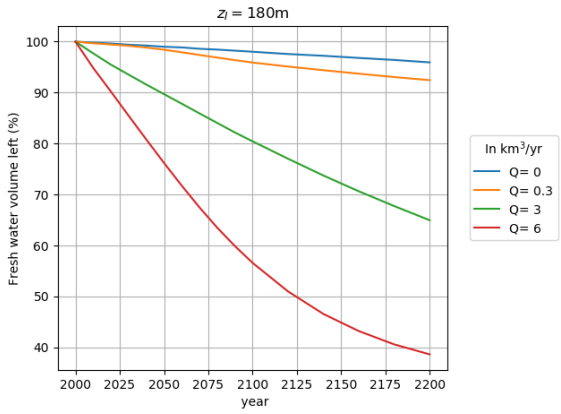

Figure 15: temporal evolution of fresh water volume for different extraction rates. The interface starts at 180 m.

Extracting Q=0.3 km^3/yr almost shows the same decay rate in fresh water volume as the Q=0 case for z=240 m. This indicates that abstractions barely exceed the supply of fresh water. This translates into the wells being in operation for a virtually infinite amount of time, without experiencing any salinization problems. This is confirmed by the time evolution of the amount of fresh water wells in Figure 16 and Figure 17. Enlarging the abstraction rates will result in (severe) decay of fresh water wells. It has to be stressed again that wells are not closed after they start to extract saline groundwater. If they would close, the salinization problem would become less severe (but on the other hand, less water can be abstracted too). For the case with z=240 m and Q= 6 km^3/yr in Figure 16, the amount of wells seems to exponentially decay towards a constant number of fresh water wells. A similar trend can be observed in Figure 14, where the fresh water volume decreases exponentially towards a steady amount. This suggests that eventually a new steady state fresh/salt water distribution will be reached. However, this would lead to a rapid closure of many wells.
For Q= 3 km^3/yr, only a small amount of wells have salinization problems. Doubling the extraction rate leads to a very rapid closure of wells compared to Q= 3 km^3/yr. For an initial interface depth of 180 m, Figure 15 and Figure 17, extracting 3 km^3/yr causes slightly more salinization problems but it still remains relatively limited. In case of Q= 6 km^3/yr, the number of fresh water wells keeps decreasing rapidly, even after 200 years.

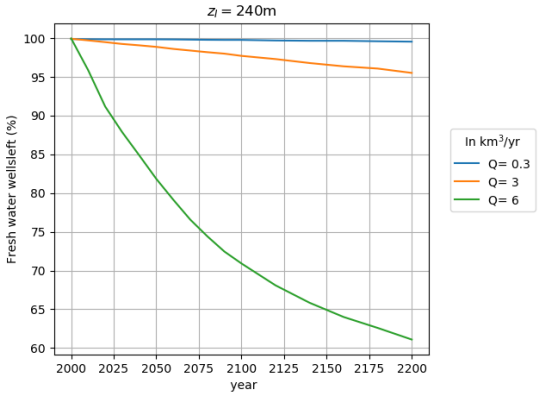

Figure 16: number of wells that still deliver fresh water versus time for different abstraction rates.

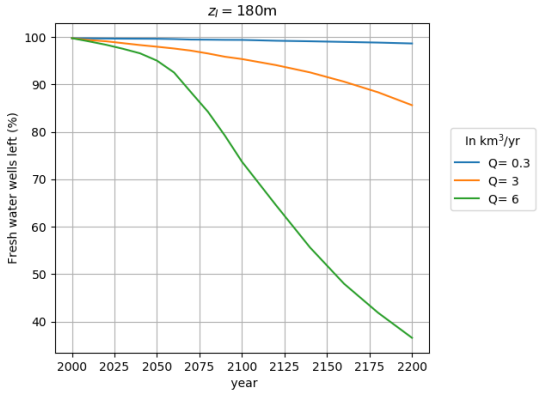

Figure 17: number of wells that still deliver fresh water versus time for different abstraction rates.

In both cases (z=240 and z=180), extracting Q=0.3 km^3/yr is closest to sustainable extractions; it does not lead to any significant closure of wells. It should be noted that extracting 6 km^3/yr led to a drawdown of 150 m in most scenarios, except for the scenario with doubled recharge and a small confining layer. Aside from salinization, this is an additional major problem since wells have to reach deeper, which is expensive.
Along with this variation in the abstraction rate, the amount that rivers infiltrate and contribute to the withdrawn groundwater changes drastically. One way to measure the contribution of the rivers, is to determine the ratio between river and recharge contributions. This ratio can be computed using the output of iMOD-SEAWAT, which returns a water budget for each stress period. For Q=0.3 km^3/yr, this ratio between rivers and recharge is approximately 4:7500, for Q=3 km^3/yr its 6:750 while for Q=6 km^3/yr its 4:75. For smaller abstraction rates, the rivers have a relatively small contribution. All these ratios are for scenario 101, with the only difference being other abstraction rates.

4.3 Influence of recharge

In our reference scenario, the upper aquifer receives 1 mm/day, equivalent to 365 mm/yr. To test the influence of recharge, a dry and a humid scenario were simulated. In Figure 18 and Figure 19 the influence of recharge on the fresh water volume is shown for a yearly abstraction rate of Q= 3 km^3/yr and initial interface depth of respectively 240 and 180 m. In Figure 20 and Figure 21 the accompanying time evolution of fresh water wells is shown. The most striking observation is the dry scenario, labelled as RCH*0.5. At a depth of 240 m, no major salinization problems occur, even for the dry scenario. On the other hand, if the interface starts at 180 m, major salinization problems will occur over the course of 200 years in the dry scenario. Another finding is that doubling the recharge has little effect. In order to better show the effect of doubling recharge, the hydraulic resistance of the confining layer was decreased. To distinguish the effect of decreasing hydraulic resistance and doubling of recharge, an additional scenario was added, labelled C*0.1. In this scenario, only the hydraulic resistance is changed with respect to the reference scenario. In another scenario, labelled C*0.1 RCH*2, the amount of recharge is doubled in addition to reducing the hydraulic resistance of the confining layer. The difference among these two scenarios was very small: doubling the recharge has little effect on the fresh/salt distribution.

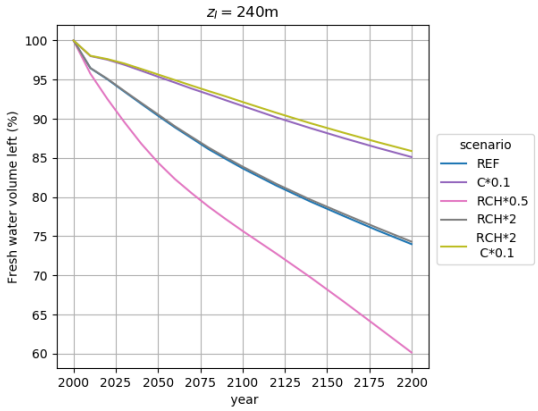

Figure 18: influence of recharge on the amount of fresh water.

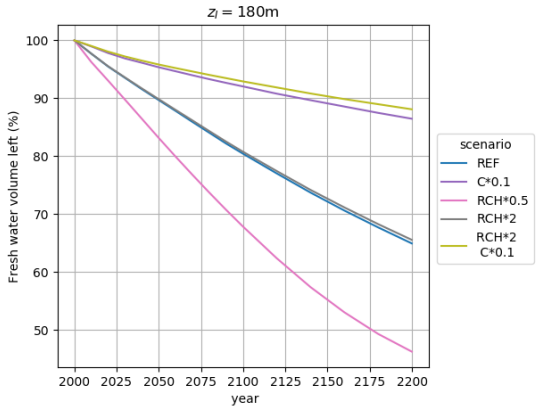

Figure 19: influence of recharge on the amount of fresh water.

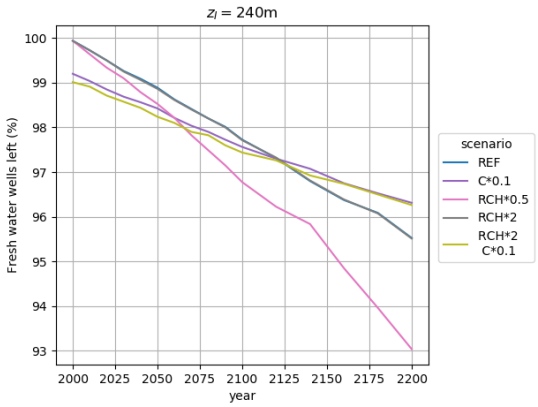

Figure 20: influence of recharge on the amount fresh water wells for Q = 6 km^3/yr, z= 240 m.

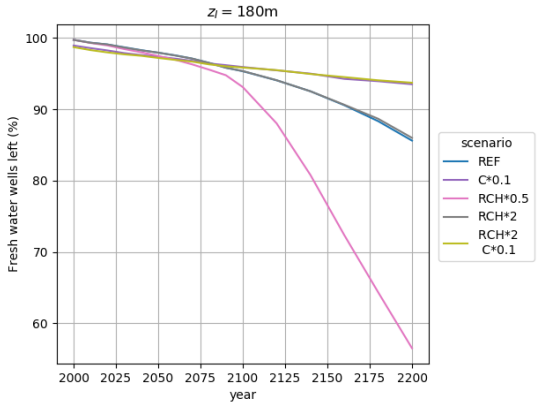

Figure 21: influence of recharge on the amount of fresh water wells for Q= 3 km^3/yr and z=180 m.

The same scenarios were investigated for a doubling of the abstraction rate: Q= 6 km^3/yr. Likewise, in Figure 22 and Figure 23, the evolution of fresh water volume is presented and in Figure 24 and Figure 25 the amount of fresh water wells.

Firstly, an important difference between the scenarios with Q= 3 km^3/yr and Q=6 km^3/yr is the much more drastic decrease in both fresh water volume and fresh water wells. In the worst case scenario, the dry scenario labelled RCH*0.5, the number of fresh water wells decreases to less than 30%. It should be noted that wells that pump saline groundwater keep on going, worsening the salinization problem.
Secondly, doubling the recharge with respect to the reference scenario greatly reduces the decay of fresh water volume as well as the number of fresh water wells.

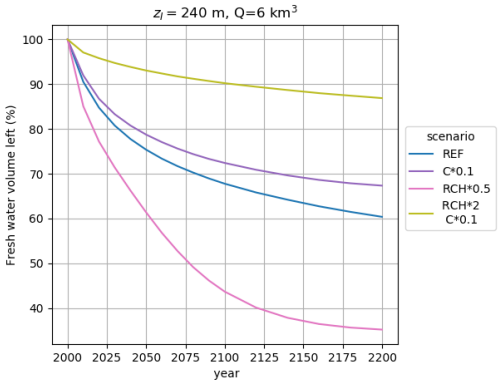

Figure 22: influence of recharge on the time evolution of the amount of fresh water.

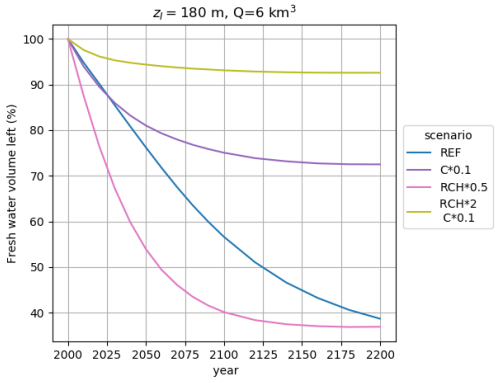

Figure 23: influence of recharge on the time evolution of the amount of fresh water.

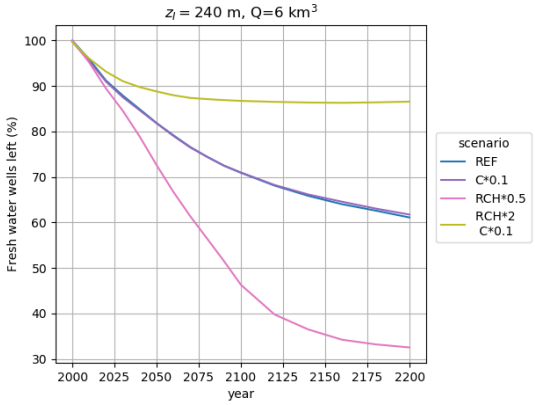

Figure 24: influence of recharge on the amount fresh water wells for Q = 6 km^3/yr, z= 240 m.

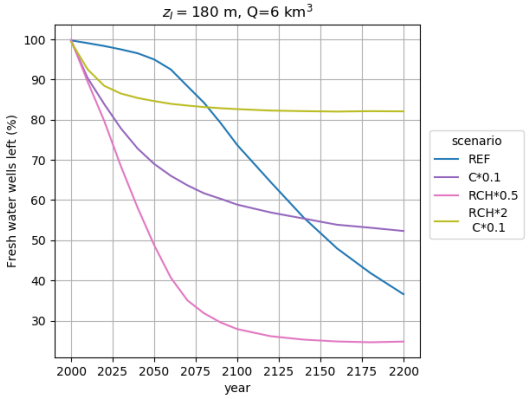

Figure 25: influence of recharge on the amount of fresh water wells for Q= 6 km^3/yr and z=180 m.

4.4 Influence of well positioning/distribution

Another factor that influences the fresh/salt distribution is the positioning or distribution of wells. Three different scenarios were deployed:

- 1: A random distribution of wells within a circle
- 2: A distribution were wells are located more towards the centre of the same circle
- 3: Same as 1, but now the circle is displaced 100 km away from the coast, instead of 50.

In Figure 28 and Figure 29 the temporal evolution of fresh water volume is depicted, in Figure 26 and Figure 27 the amount of fresh water wells. In general, for the case where the city is placed 100 km away from the coast, no or less severe salinization problems occur. In case the city centre is just 50 km away from the coast, the abstractions will interact with the saline groundwater from the sea. In other words, salt water intrusion is accelerated by the abstractions. Abstractions that are more focussed towards the city centre will lead to the fastest closure of wells. However, this does not translate into the fastest drop in fresh water volume.

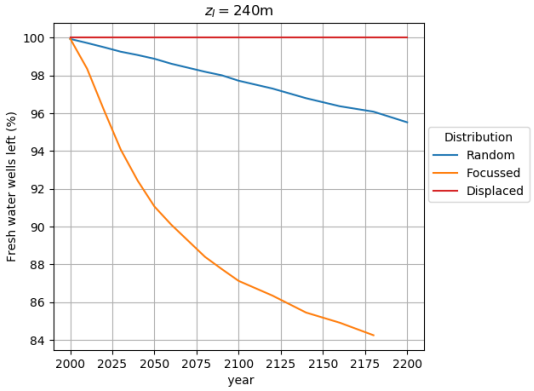

Figure 26: influence of well positioning on the fresh water volume. 'Displaced' corresponds to the city being located 100 km from the coast, instead of 50 km.

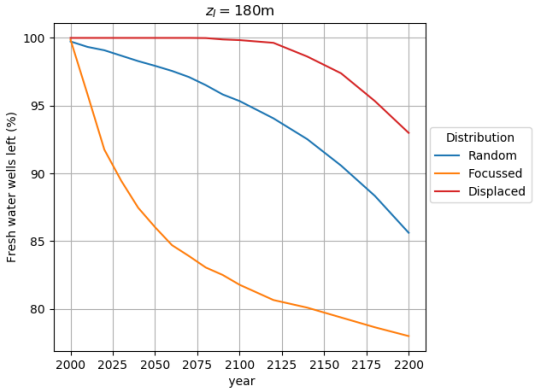

Figure 27: influence of well positioning on the fresh water volume. 'Displaced' corresponds to the city being located 100 km from the coast, instead of 50 km.

Since most abstractions are more focussed towards the city centre, the distance towards the sea is also larger. Therefore, less interaction with the fresh/salt water interface close to the sea occurs. In the case where the abstractions are random, more wells are closer to the sea, which tends to accelerate salt water intrusion. This is also the reason that the scenario with the city being located 100 km away from the coast does not experience any salinization problems for z=240 m, see Figure 26.
Furthermore, since most abstractions take place on a smaller scale, salinization effects will also be more local. Eventually, the scenario where the city is displaced will catch up with the scenario of more abstractions in the centre, see Figure 29.

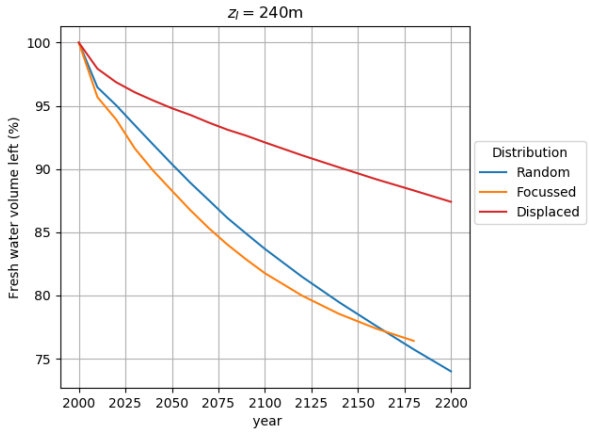

Figure 28: influence of well positioning on the fresh water volume.

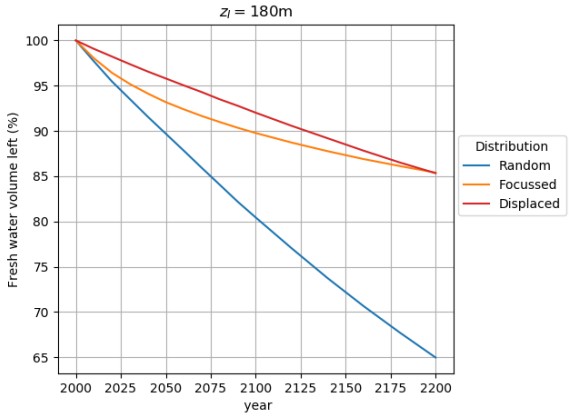

Figure 29: influence of well positioning on the fresh water volume for initial interface depth of 180 m.

4.5 Influence of initial interface depth

Lastly, the influence of the initial interface depth was examined. If we consider Figure 30, the amount of fresh water responds differently at different starting depths. A clay layer is located at a depth of 150 m, confining the aquifer below. This may explain the more linear decay if the saline groundwater is only located in the aquifer below the clay layer. It has to prograde through the clay layer to salinify the aquifer on top. Above the clay layer, in the upper aquifer, the saline groundwater experiences more interaction with the layer close to the surface, explaining the non-linear decay.

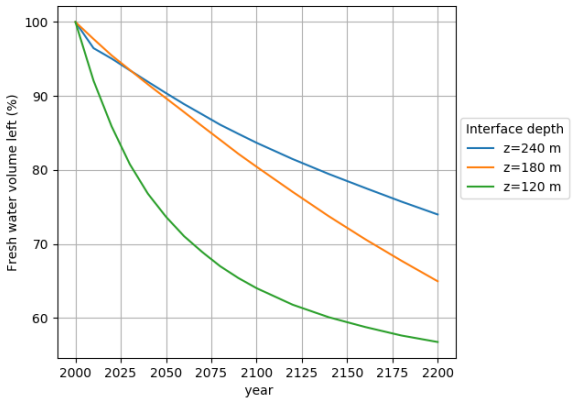

Figure 30: influence of the initial depth of the interface on the evolution of fresh water volume. Abstraction rate is Q=3 km^3/yr in all cases.

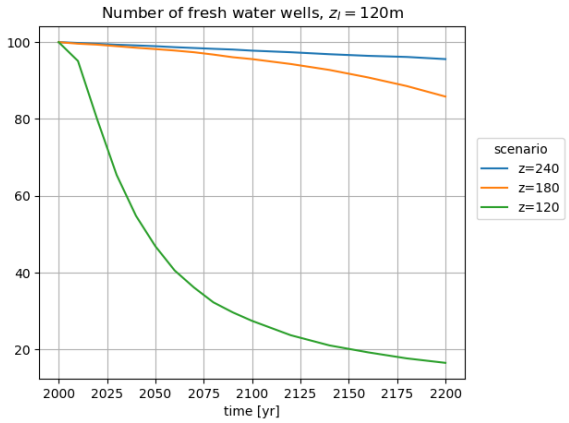

Figure 31: influence of the initial depth of the interface on the evolution of fresh water volume. Abstraction rate is Q=3 km^3/yr in all cases.

Extracting Q = 3 km^3/yr while the saline groundwater is located at a depth of 120 m, leads to a tremendous closure of wells. However, it seems that the fresh/salt water distribution evolves towards a steady state after 200 years. Areas where no wells are presented apparently remain fresh and seem to stay fresh, despite wells being active in the surroundings.
It should be stressed again that 240, 180 and 120 m are the depths were the saline groundwater (C = 35 g/L) ended and where the interface started. At a depth of respectively 225, 165 and 105 m, the groundwater was perfectly fresh again (C=0 g/L). This configuration of the fresh/salt distribution was used to initialize the model in order to find an approximate steady state of the fresh/salt distribution without any extractions. Subsequently, after the approximate steady state was reached, the saline groundwater (with C> 1 g/L) reached a depth of respectively 217.5, 172.5 and 90 m.

4.6 Overview of all scenarios and groundwater flow

In Figure 32, Figure 33 and Figure 37 an overview is given of all the scenarios for an initial interface depth of respectively 240, 180 and 120 m. At a depth of 120 m, not all the scenarios were simulated successfully, since the model crashed sometimes. A reason for this was not yet identified due to a lack of time.
A striking difference between the three graphs is the y-scale. While in most scenarios for z=240 m and z=180 m only at most 10% of the wells experience salinization problems, this is drastically different for z=120 m. Abstracting 3 km^3/yr leads to massive salinization problems of wells, in some cases even half of the total amount in just 40 years.

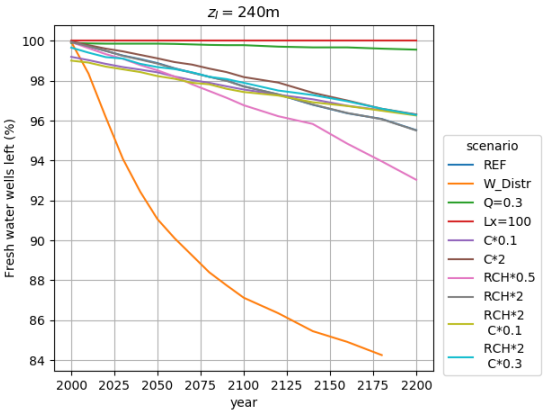

Figure 32: overview of all scenarios that start with an initial interface depth of 240 m. Q= 3 km^3/yr unless noted otherwise.

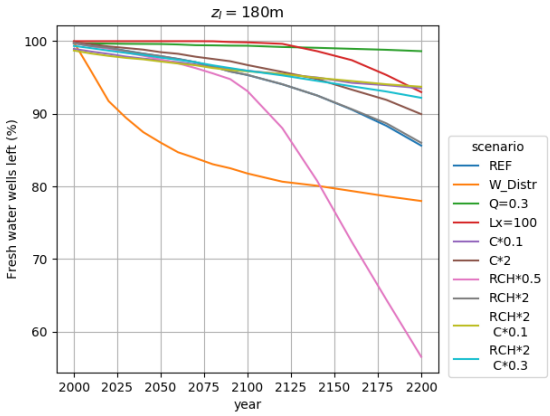

Figure 33: overview of all scenarios that start with an initial interface depth of 180 m. Q= 3 km^3/yr unless noted otherwise.

Apart from the intensification of salinization problems with the interface located closer to the surface, some particular scenarios draw the attention. For z=180 m only in arid areas severe salinization problems will occur. Other than this, only a high spatial density of abstractions poses significant salinization problems.
Nevertheless, for z=240 m and z=180 m it can be concluded that salinization problems are in most other scenarios not widespread and very limited on a timescale of 200 years.

Additionally, Figure 34 - Figure 36 illustrate the difference in groundwater flow between respectively a dry scenario (107), the reference scenario (101) and a humid scenario (109). In a humid climate with a small confining layer, Figure 36, most withdrawn groundwater directly comes from recharge. For a dry climate, less recharge is available and it has to come from elsewhere, Figure 34.

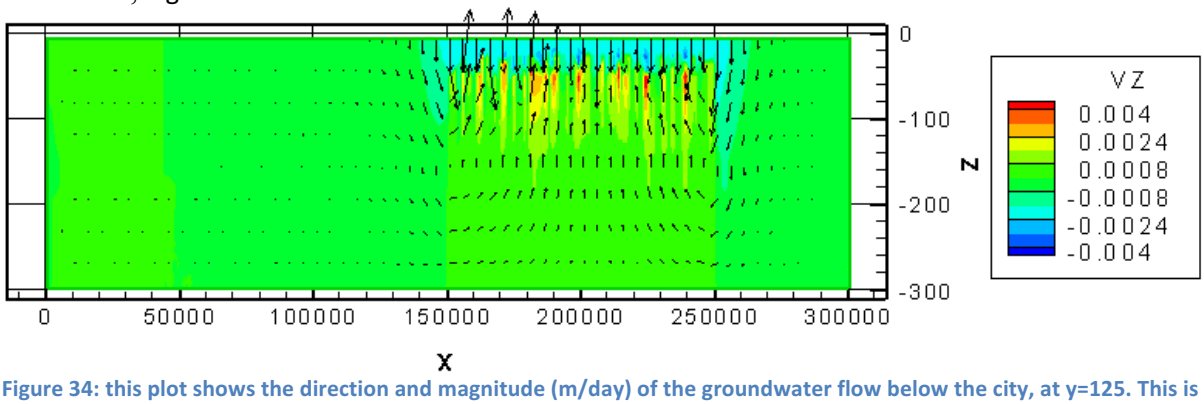

Figure 34: this plot shows the direction and magnitude (m/day) of the groundwater flow below the city, at y=125. This is for the dry scenario (107), labelled as RCH*0.5 in other graphs.

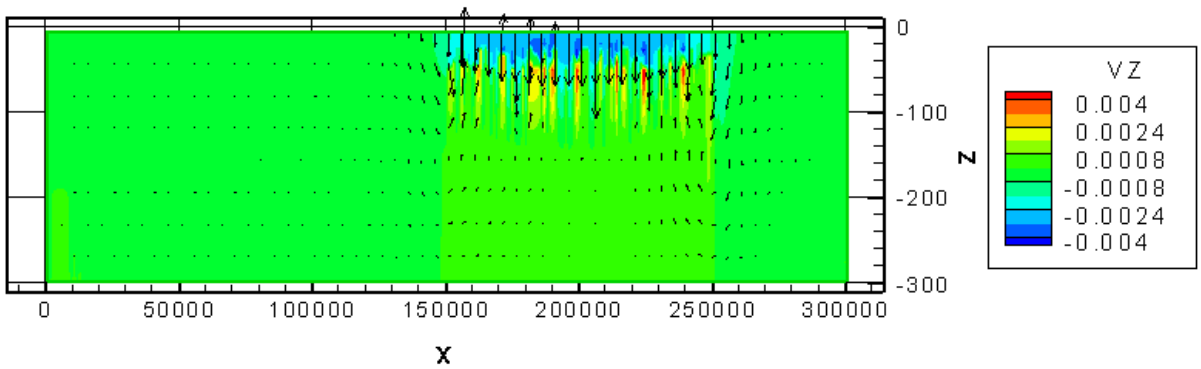

Figure 35: this plot shows the direction and magnitude of the groundwater flow below the city, at y=125. This is for the reference scenario (101), labelled as REF. In color the magnitude (m/day) of the vertical component of the velocity is shown.

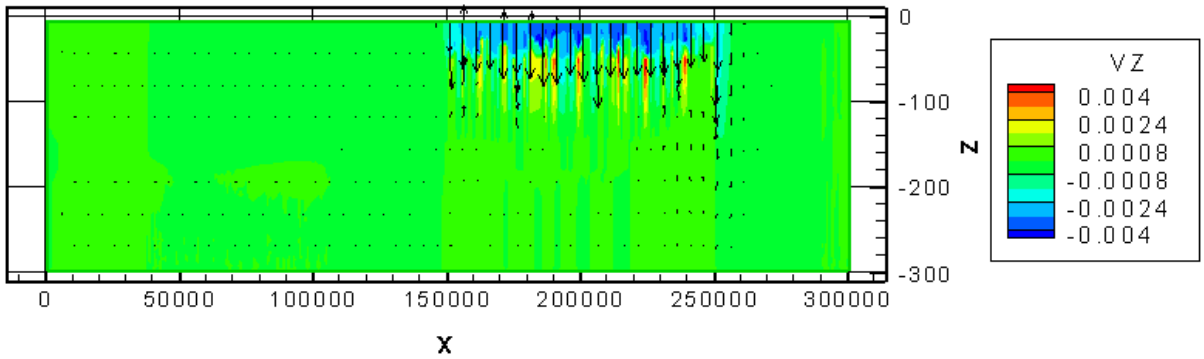

Figure 36: this plot shows the direction and magnitude (m/day) of the groundwater flow below the city, at y=125. This is for scenario 109, also labelled as RCH*2 C*0.1, which has a humid climate and a small confining layer. In colors again the vertical component of the velocity is shown.

For z=120 m (where brackish water actually already starts at 90 m depth), major salinization problems will occur on a short timescale of only 40 years. After 40 years, half of the wells experience salinization problems. Obviously, this can and will be delayed in reality by turning wells off the moment they pump saline groundwater. However, this also forces the government to pump water from elsewhere.

An additional layer of clay (labelled as C*2 in Figure 37) will delay the salinization problem but not prevent it.

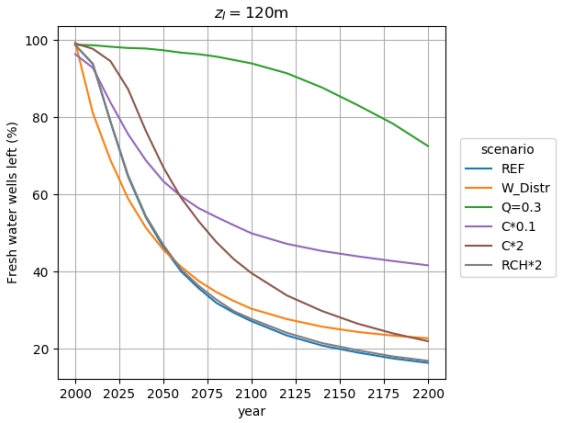

Figure 37: overview of all scenarios that start with an initial interface depth of 120 m and did not crash. Q= 3 km^3/yr unless noted otherwise.

Lastly, the difference in percentage of fresh water wells left between a thick (labelled as REF) and a thin confining layer (C*0.1) is slightly more than 20% after 100 years, increasing to 25% after 200 years. The scenario with C=5000 days was not successfully simulated and is missing from Figure 37.

5 Discussion/Conclusion

Before embarking on discussing the results, a few important notes are stated. The results have mostly a qualitative value rather than quantitative. No time dependent well management was used: wells continued to pump even if saline groundwater was encountered. In one scenario, however, wells were turned off after the groundwater became saline. Results from this scenario showed that about 50% of the wells were closed over time. In this way salinization was delayed but with this inevitably comes also a 50% decrease in groundwater yield over the course of 200 years. In a world with growing water demand and climate change, the groundwater withdrawal can be expected to increase too. In many of the scenarios discussed below, salinization problems will cause a tremendous decrease of groundwater yield. In the future this will result in major problems regarding finding suitable water. Hence, knowledge on the dominant physical mechanisms behind salinization can be used to prevent or reduce salinization problems. In this section the results are summarized and grouped based on themes and subsequently, physical mechanisms are discussed.

5.1 Confining layer

The influence of a confining layer was investigated by varying its hydraulic resistance (C). If the saline groundwater was located at z=240 m, i.e. below the aquitard at z=150 m, there was no difference between respectively a thin and thick confining layer with respect to the number of fresh water wells. For z=180 m, 15% more wells experienced salinization problems for a thick confining layer compared to a thin layer on a timescale of 200 years. For z=120 m, this increases to 25%. The influence of the confining layer amplifies if the saline groundwater is located at a more shallow level. If the saline groundwater is located very deep and is still below the aquitard, it reacts weakly to changes in the upper subsurface.

5.2 Abstraction rate

The evolution of fresh water volume was tested using three different abstraction rates: Q=0.3 km^3/yr, Q=3 km^3/yr and Q= 6 km^3/yr. From the results it became clear that extracting 0.3 km^3/yr is almost perfectly sustainable in terms of fresh water volume and the number of fresh water wells that remain operable. Little or no upconing of saline groundwater happened: sufficient recharge in the upper aquifer is able to compensate the withdrawal of groundwater. On top of this, the aquitard at z=150 m prevents a rapid upconing of saline groundwater. For the scenarios with initial interface depth of z=180 m and z=240 m. Only for the scenario where the initial interface was located at z=120 m, a drop in fresh water wells of slightly more than 20% is observed over the course of 200 years. In that case, no aquitard is present to shield the saline groundwater and horizontal flow cannot prevent upconing.

While extracting 0.3 km^3/yr has small salinization risks, extracting 6 km^3/yr is not feasible. It will lead to a drawdown of approximately 150 m and even for the scenarios with z=240 m to significant salinization problems. Extracting this amount is groundwater mining and may only be done in deltaic areas with high recharge amounts and no (or small) confining layer.

5.3 Recharge & rivers

In dry areas, where recharge is half of the reference scenario, significant salinization problems will occur for z=180 m. In both cases (z=240 m and z=180 m) a severe drop in total fresh water volume is observed, however for z=240 m the saline groundwater barely reaches the wells on this timescale. Due to the abstractions groundwater level drops to 15 meters below sea level: recharge does not suffice.
In very humid areas, where both recharge and river conductance are doubled with respect to the reference scenario, barely any increase in fresh water volume and fresh water wells is observed. This amount of recharge will lead to a surplus of water, which will be transported away by drains and the river network.
However, if the abstraction rate is increased in this scenario, doubling of the recharge and river conductance tremendously slows down salinization. Instead of the reference scenario where more than 60% of the wells experiences salinization problems, less than 20% does so in this case. On top of an increased recharge, rivers and ditches are able to infiltrate more effectively because the confining layer is of little importance (small hydraulic resistance).

5.4 Well distribution

Abstracting groundwater on a small area in the city centre, which is located 50 km from the sea, leads to largest closure of wells. However, if most of the wells are located in the city centre, only a few other wells are close to the sea. The wells in the city centre seem disconnected from the sea: these wells don't accelerate salt water intrusion much. Nevertheless, this will lead to local salinization problems in the city centre due to upconing of saline groundwater. Abstracting only in the city centre naturally leads to more local salinization problems, it seems the fresh/salt water distribution evolves towards a new steady state. However, in that case all wells located in the city centre have to close.
Interestingly, if the wells are distributed randomly over the circular urban area, this leads to the most rapid drop in fresh water volume. In the latter case many wells are located close to the sea and this accelerates salt water intrusion. Abstracting 3 km^3/yr at a distance of 100 km from the coast prevents any salt water intrusion problems.
Concluding, abstracting groundwater within 50 km from the sea will accelerate salt water intrusion, while making abstractions over a larger area instead in the city centre will delay salinization problems.

5.5 Depth of interface

Salinization problems are minor at a timescale of 200 years if the aquitard at a depth of 150 m shields the saline groundwater below. However, if saline groundwater is present above the aquitard, very rapid salinization occurs. It is not necessarily the depth of the interface which is important but more the position of the interface with respect to the geology.

5.6 A note on physical mechanisms driving salinization

From this research a rough estimation can be given on the dominant physical mechanisms that drive (or delay) salinization. Most of these mechanisms interact with each other and are not independent.
From the results, it became clear that the degree and speed of salinization was in most cases very sensitive to recharge amounts. If no or little recharge is available, a large part of the withdrawn groundwater has to be supplied from horizontal flow, or from below, accelerating the upconing of saline groundwater. This is clearly visible when comparing the dry scenario

in Figure 34 with respectively the reference and humid scenario, Figure 35 and Figure 36. In the dry scenario groundwater flow has a significant upward component, which is absent in the other two cases. However, the amount of recharge available for groundwater uptake by wells, is determined by the (absence or presence of a) confining layer. For example, if a firm confining layer is present, a high recharge rate has little influence. The combination of both recharge amount (i.e. climate type) and the presence of a confining layer greatly influences the salinization speed. In most cases, river contributions to the withdrawn groundwater were relatively small compared to recharge: usually the ratio between them was around 4:750. The only factor that made the river contribution significant with respect to recharge, was the abstraction rate. If the abstraction rate increased from 0.3 km^3/yr to 6 km^3/yr, the river contribution increased by a factor 100, whereas a smaller confining layer only doubled the river infiltration. Therefore, only in the case of high abstraction rates, rivers seem to be significant with respect to recharge.

Another factor is geology, in particular the presence of aquitards. Aquitards will shield the saline groundwater for a finite amount of time. The intensity of salinization has a highly nonlinear response to the location of the interface with respect to aquitards (visible in Figure 31). The strength of the response depends on whether the abstraction rate is too high for this aquifer system or not. The evolution of the salinization problem as function of abstraction rates is presented in Figure 14 and Figure 15. This indicates that abstracting Q=0.3 km^3/yr is safe on a timescale of 200 years. Furthermore, abstracting far enough from the sea (at least 50 km) will prevent salt water intrusion from intensifying salinization (at least on a timescale of 200 years).

5.7 Comparison to real deltaic areas

Even though a conceptual model was used and the scenarios developed are completely synthetic, they are based on real deltaic areas. In some cases, real deltaic areas may share some (or a lot) of the same characteristics of particular scenarios. If this is the case, the results for these scenarios can provide an indication on the intensity of future salinization problems. Below, a deltaic area, e.g. the Mekong Delta (MKD) is matched with a particular scenario. The MKD shares many similarities with scenario 208, labelled as RCH*2 in Figure 37. The similarities between the MKD and 208 are listed below:

- Both have a thick confining layer on top
- MKD has a humid climate and 208 experiences relatively high recharge amounts too
- Due to the humid (synthetic) climate, both have a dense network of channels/rivers
- Both have saline groundwater in the upper aquifer (except for the upper part of MKD)

However, there are some differences. In the lower part of the MKD, salinization takes place at very shallow depths: in large areas the whole aquifer is even completely salinized.
In addition, the abstraction rate in MKD (close to 1 km^3/yr) is smaller than in scenario 208 (3 km^3/yr). It also has to be noted again that in scenario 208 the wells continued pumping even in case saline groundwater was encountered. The thick confining layer is the restrictive factor in this scenario: it diminishes recharge to the upper aquifer. Based on this, groundwater uptake won't be fuelled by recharge much and this delta is more likely vulnerable to salinization problems.

As becomes clear from Figure 37, significant salinization problems will occur on a timescale of 50 years for scenario 208. By that time, half of the wells experience salinization problems. However, as became clear from Figure 9, the salinization problem can be delayed if wells are turned off. Nevertheless, even if the wells are turned off, still half of the wells can be closed an additional 40 or 50 years later. In the MKD the abstraction rate is smaller than in scenario 208, but in the MKD salinization (mostly) does occur at more shallow depths. The presence of the interface at more shallow depths will counteract the positive effect of a smaller abstraction rate. This complicates matters, but a rough first estimate would be that half of the wells are closed by 2100. However, if the abstraction rate increases due to increase in groundwater withdrawal or droughts/climate change, salinization will be even more rapid.

From the simulations of the different scenarios, it became clear that in many cases significant salinization problems will occur. However, the severity of salinization depends on many factors, most notably recharge rates and confining layer, that interact with each other. In many cases too large amounts are extracted, resulting in major salinization problems on a timescale of 100 years or less. Due to this, many wells have to close because they will soon pump saline groundwater. This results in a decrease of groundwater withdrawal over time. This research gives an overview of the physical mechanisms and a first order estimate of the timescale at which salinization will occur, based on conceptual models. Knowledge on physical mechanisms driving salinization and the ability to predict salinization problems can be essential in light of climate change and the ever increasing water demand.

References:

Abam, T. K. S. (2001). Perspectives de la recherche hydrologique régionale dans le delta du Niger. *Hydrological Sciences Journal*, *46*(1), 13–25. https://doi.org/10.1080/02626660109492797

Antonellini, M., Mollema, P., Giambastiani, B., Bishop, K., Caruso, L., Minchio, A., … Gabbianelli, G. (2008). Salt water intrusion in the coastal aquifer of the southern Po Plain, Italy. *Hydrogeology Journal*, *16*(8), 1541–1556. https://doi.org/10.1007/s10040-008-0319-9

Arabi, N.E. (2012). Environmental Management of Groundwater in Egypt via Artificial Recharge Extending the Practice to Soil Aquifer Treatment (SAT). *International Journal of Environment and Sustainability*, *1*(3), 66–83. https://doi.org/10.24102/ijes.v1i3.91

Barlow, P. M., & Reichard, E. G. (2010). L'intrusion d'eau salée dans les régions côtières d'Amérique du Nord. *Hydrogeology Journal*, *18*(1), 247–260. https://doi.org/10.1007/s10040-009-0514-3

Bui, D. Du, Kawamura, A., Tong, T. N., Amaguchi, H., Nakagawa, N., & Iseri, Y. (2011). Identification of aquifer system in the whole Red River Delta, Vietnam. *Geosciences Journal*, *15*(3), 323–338. https://doi.org/10.1007/s12303-011-0024-x

Buschmann, J., Berg, M., Stengel, C., Winkel, L., Sampson, M. L., Trang, P. T. K., & Viet, P. H. (2008). Contamination of drinking water resources in the Mekong delta floodplains: Arsenic and other trace metals pose serious health risks to population. *Environment International*, *34*(6), 756–764. https://doi.org/10.1016/j.envint.2007.12.025

Colombani, N., Cuoco, E., & Mastrocicco, M. (2017). Origin and pattern of salinization in the Holocene aquifer of the southern Po Delta (NE Italy). *Journal of Geochemical Exploration*, *175*, 130–137. https://doi.org/10.1016/j.gexplo.2017.01.011

Custodio, E. (2002). Aquifer overexploitation: What does it mean? *Hydrogeology Journal*, *10*(2), 254–277. https://doi.org/10.1007/s10040-002-0188-6

de Montety, V., Radakovitch, O., Vallet-Coulomb, C., Blavoux, B., Hermitte, D., & Valles, V. (2008). Origin of groundwater salinity and hydrogeochemical processes in a confined coastal aquifer: Case of the Rhône delta (Southern France). *Applied Geochemistry*, *23*(8), 2337–2349. https://doi.org/10.1016/j.apgeochem.2008.03.011

Goni, I., Edet, A., Olasehinde, P., Bale, R., Adelana, S., & Vrbka, P. (2008). An overview of the geology and hydrogeology of Nigeria, (September). https://doi.org/10.1201/9780203889497.ch11

Hoque, M. A., Burgess, W. G., Shamsudduha, M., & Ahmed, K. M. (2011). Delineating low-arsenic groundwater environments in the Bengal Aquifer System, Bangladesh. *Applied Geochemistry*, *26*(4), 614–623. https://doi.org/10.1016/j.apgeochem.2011.01.018

Jasechko, S. (2014). The pronounced seasonality of globabl grounwater recharge, 8845–8867. https://doi.org/10.1002/2014WR015809

Konikow, L. F. (2015). Long-Term Groundwater Depletion in the United States. *Groundwater*, *53*(1), 2–9. https://doi.org/10.1111/gwat.12306

Kotchoni, D. O. V., Vouillamoz, J. M., Lawson, F. M. A., Adjomayi, P., Boukari, M., & Taylor, R. G. (2018). Relationships between rainfall and groundwater recharge in seasonally humid Benin: a comparative analysis of long-term hydrographs in sedimentary and crystalline aquifers. *Hydrogeology Journal*, 1–11. https://doi.org/10.1007/s10040-018-1806-2

Kumar, B., Rao, M. S., Gupta, a K., & Purushothaman, P. (2011). Groundwater management in a coastal aquifer in Krishna River Delta , South India using isotopic approach, *100*(7).

Lackey, G., Neupauer, R. M., & Pitlick, J. (2015). Effects of streambed conductance on

stream depletion. *Water (Switzerland)*, *7*(1), 271–287. https://doi.org/10.3390/w7010271
MacDonald, A. M. et al. (2013). Groundwater resources in the Indo - Gangetic Basin. *International Conference on Advances in Water Resources Development and Management (AWRDM-2013) 23rd – 27th October, 2013*, (October 2014).
Mahmud, M. I., Sultana, S., Hasan, M. A., & Ahmed, K. M. (2017). Variations in hydrostratigraphy and groundwater quality between major geomorphic units of the Western Ganges Delta plain, SW Bangladesh. *Applied Water Science*, *7*(6), 2919–2932. https://doi.org/10.1007/s13201-017-0581-x
McDonald, M. G., & Harbaugh, A. W. (1988). A modular three-dimensional finite-difference groundwater flow model, Techniques of Water-Resources Investigations Report, 06-A1. *Methods for Determination of ...*, 588. https://doi.org/10.1016/0022-1694(70)90079-X
Minderhoud, P., Erkens, G., Pham, V. H., Vuong, B. T., & Stouthamer, E. (2016). To drink or to drown? Impact of groundwater extraction on subsidence in the Mekong Delta, Vietnam, *9*(2014), 2015.
Naganna, S. R., Deka, P. C., Ch, S., & Hansen, W. F. (2017). Factors influencing streambed hydraulic conductivity and their implications on stream–aquifer interaction: a conceptual review. *Environmental Science and Pollution Research*, *24*(32), 24765–24789. https://doi.org/10.1007/s11356-017-0393-4
Post, V., Kooi, H., & Simmons, C. (2007). Using hydraulic head measurements in variable-density ground water flow analyses. *Ground Water*, *45*(6), 664–671. https://doi.org/10.1111/j.1745-6584.2007.00339.x
Radhakrishna, I. (2001). Saline fresh water interface structure in Mahanadi delta region , *40*(January).
Sahoo, S., & Jha, M. K. (2017). Numerical groundwater-flow modeling to evaluate potential effects of pumping and recharge: implications for sustainable groundwater management in the Mahanadi delta region, India. *Hydrogeology Journal*, 2489–2511. https://doi.org/10.1007/s10040-017-1610-4
Sherif, M., Sefelnasr, A., & Javadi, A. (2012). Incorporating the concept of equivalent freshwater head in successive horizontal simulations of seawater intrusion in the Nile Delta aquifer, Egypt. *Journal of Hydrology*, *464–465*, 186–198. https://doi.org/10.1016/j.jhydrol.2012.07.007
Wada, Y., van Beek, L. P. H., & Bierkens, M. F. P. (2011). Modelling global water stress of the recent past: on the relative importance of trends in water demand and climate variability. *Hydrology and Earth System Sciences*, *15*(12), 3785–3808. https://doi.org/10.5194/hess-15-3785-2011
Wada, Y., Van Beek, L. P. H., & Bierkens, M. F. P. (2012). Nonsustainable groundwater sustaining irrigation: A global assessment. *Water Resources Research*, *48*(1). https://doi.org/10.1029/2011WR010562
Wada, Y., Van Beek, L. P. H., Van Kempen, C. M., Reckman, J. W. T. M., Vasak, S., & Bierkens, M. F. P. (2010). Global depletion of groundwater resources. *Geophysical Research Letters*, *37*(20), 1–5. https://doi.org/10.1029/2010GL044571
Wada, Y., Wisser, D., & Bierkens, M. F. P. (2014). Global modeling of withdrawal, allocation and consumptive use of surface water and groundwater resources. *Earth System Dynamics*, *5*(1), 15–40. https://doi.org/10.5194/esd-5-15-2014
Zhang, Y., Xue, Y. Q., Wu, J. C., Ye, S. J., Wei, Z. X., Li, Q. F., & Yu, J. (2007). Characteristics of aquifer system deformation in the Southern Yangtse Delta, China. *Engineering Geology*, *90*(3–4), 160–173. https://doi.org/10.1016/j.enggeo.2007.01.004
Zhu, X. B., Wu, J. C., Wu, J. F., & Ye, S. J. (2011). Optimization of groundwater pumping subsidence in the Yangtze Delta , China, (September 2009), 2011.